In-Flight Calibration Methods for Temperature-Dependent Offsets in the MMS Fluxgate Magnetometers
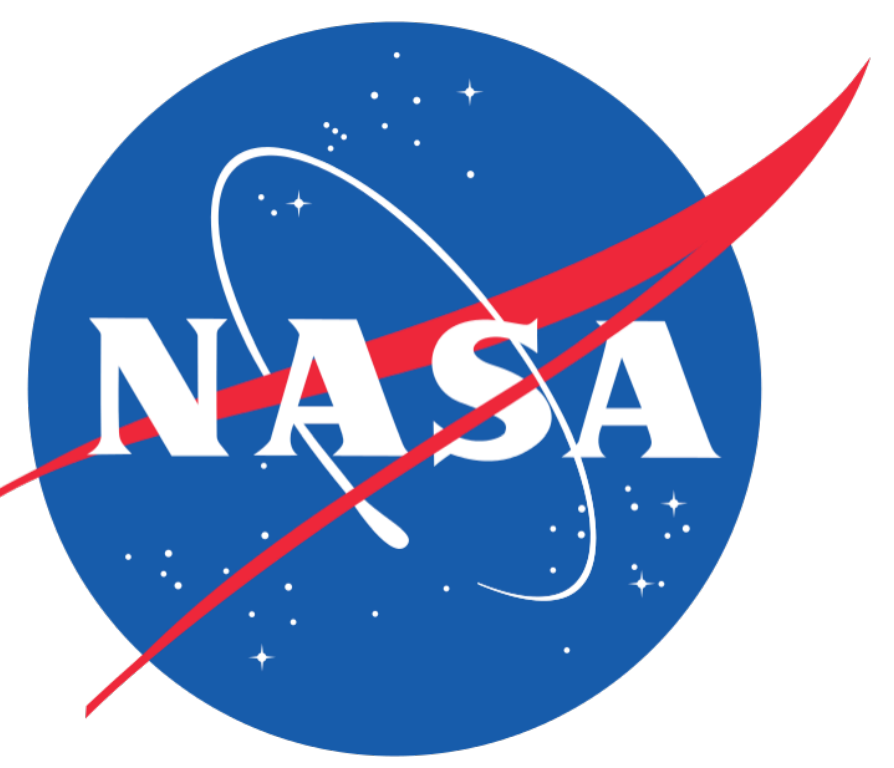
K. R. Bromund[1], F. Plaschke[2], R. J. Strangeway[3], B. J. Anderson[4], B. G. Huang[1,7],
W. Magnes[2], D. Fischer[2], R. Nakamura[2], H. K. Leinweber[3], C. T. Russell[3],
W. Baumjohann[2], M. Chutter[5], R. B. Torbert[5], G. Le[1], J. A. Slavin[6], E. L. Kepko[1]

SM21A-2455

[1]NASA Goddard Space Flight Center (GSFC)
[2]Space Research Institute (IWF), Austrian Academy of Sciences
[3]University of California Los Angeles (UCLA)
[4]Johns Hopkins University Applied Physics Laboratory
[5]University of New Hampshire
[6]University of Michigan Ann Arbor
[7]ADNET Systems, Inc.

For more information, contact
kenneth.r.bromund@nasa.gov

Abstract

During the first dayside season of the Magnetospheric Multiscale (MMS) mission, the in-flight calibration process for the Fluxgate magnetometers (FGM) implemented an algorithm that selected a constant offset (zero-level) for each sensor on each orbit. This method was generally able to reduce the amplitude of residual spin tone to less than 0.2 nT within the region of interest (ROI). However, there are times when the offsets do show significant short-term variations. These variations are most prominent in the nighttime season (phase 1X), when eclipses are accompanied by offset changes as large as 1 nT. Eclipses are followed by a recovery period as long as 12 hours where the offsets continue to change as temperatures stabilize. Understanding and compensating for these changes will become critical during Phase 2 of the mission in 2017, when the nightside will become the focus of MMS science. Although there is no direct correlation between offset and temperature, the offsets are seen — for the period of any given week — to be well-characterized as a function of instrument temperature. Using this property, a new calibration method has been developed that has proven effective in compensating for temperature-dependent offsets in the spin plane during phase 1X of the MMS mission and also promises to further refine calibration quality during the dayside seasons.

Background

- The general approach to the MMS FGM calibration is presented in (Russell, et al. 2014).
- Details of the original calibration process that was used for Phase 1A and the beginning of Phase1X were described by (Bromund, Leinweber, Plaschke, et al 2015):
  - 12 independent parameters of: offset (3), differential spin-plane gain (1), spin-axis alignment (2), non-orthogonality (3), absolute gain (2), absolute phase (1).
  - Reliable dynamic estimates of parameters over the course of an orbit.
  - Final results were orbit-averages of the dynamic estimates.
- In the first year of science operations, of the 12 parameters, the 2 spin-plane offsets (derived by the original method described in the box below) have clearly shown the most significant variability on both short- and long-term time scales.
- The current study is restricted to low-field range, where offsets dominate the calibration.
- The performance of the original method is illustrated in two example weeks, shown in Fig. 1 and Fig. 2, representing dayside (Phase 1A) and nightside (Phase 1X), respectively.
- Temperature-dependent offsets are developed and results presented for both examples.

Dayside Example, Phase 1A

- No eclipses within low-field range (Fig. 1).
- Negligible variation within the ROI for both temperature (~ 0.5 °C) and offset (< 0.1 nT).
- Minimal (~ 5 °C) temperature variation, accompanied by ≤ 0.2 nT offset variation, consistently seen in the outbound leg of each orbit.
- Can achieve goal of 0.100 nT accuracy within the ROI using orbit-constant offsets.
- Prolonged geophysical activity within the ROI limits the available statistics. In other examples, this occasionally leads to errors ~ 0.100 nT in the ROI.

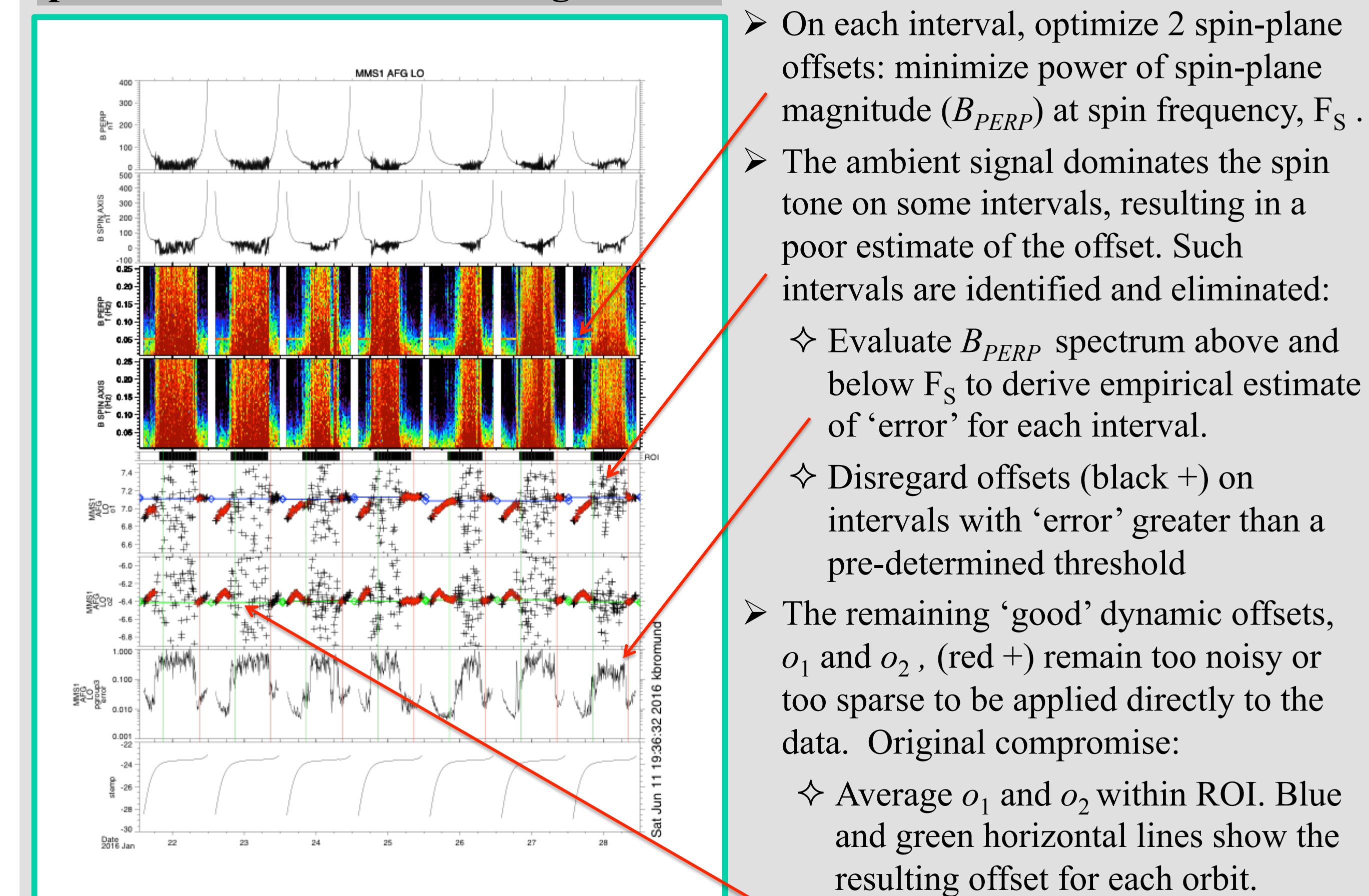**Review: Calibration method for spin-plane offsets in low-field range**

- Divide each orbit into ~15 minute intervals
- On each interval, optimize 2 spin-plane offsets: minimize power of spin-plane magnitude (B_{PERP}) at spin frequency, F_S.
- The ambient signal dominates the spin tone on some intervals, resulting in a poor estimate of the offset. Such intervals are identified and eliminated:
  - Evaluate B_{PERP} spectrum above and below F_S to derive empirical estimate of 'error' for each interval.
  - Disregard offsets (black +) on intervals with 'error' greater than a pre-determined threshold
- The remaining 'good' dynamic offsets, o_1 and o_2, (red +) remain too noisy or too sparse to be applied directly to the data. Original compromise:
  - Average o_1 and o_2 within ROI. Blue and green horizontal lines show the resulting offset for each orbit.
  - Use average value from previous orbit, in case of insufficient statistics.

Fig. 1. Low-range calibration diagnostic, for typical week of Phase 1A: 21-28 January, 2016

The Effect of Eclipses

Nightside Example, Phase 1X

- Constant offsets fail to remove spin tone during and after eclipses.
  - Dynamic offsets differ from the orbit average by 0.3 – 0.5 nT for a significant time after eclipse.
- As the shadow season progresses, these effects dominate the ROI.
  - Shadow moves towards apogee.
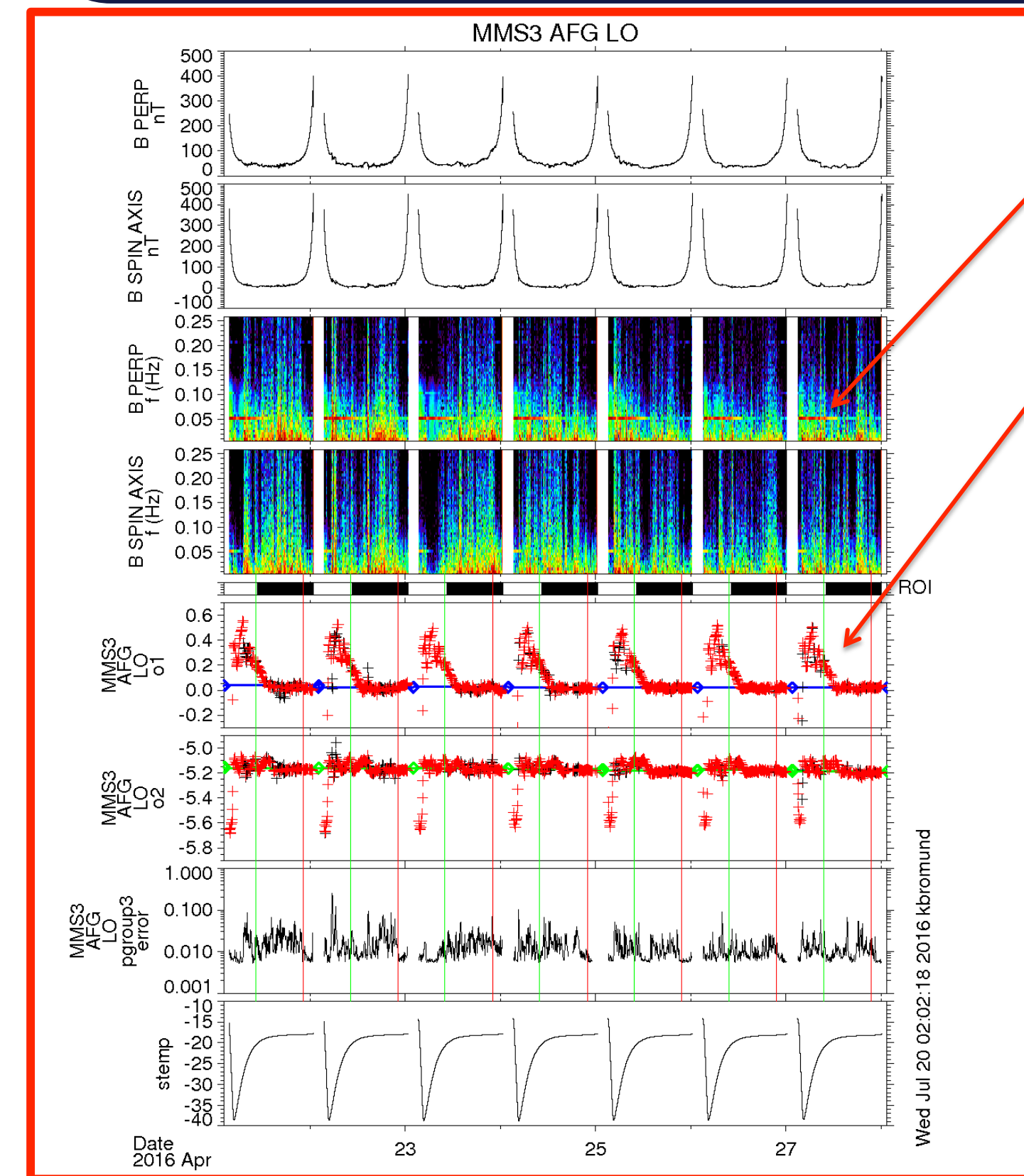 - Duration of shadow increases, with corresponding increase in recovery time and associated offset variations.

Fig. 2. A typical week during Phase 1X: 21-27 April, 2016. Note the range of sensor temperature, $T_S(t)$, (bottom panel) is ~25 °C (compared to 5 °C in Fig. 1)

Temperature Dependence

- In Fig. 1 and Fig. 2, the dynamic offsets and the sensor temperature appear to follow a consistent pattern from orbit to orbit, suggesting a causal relationship.

- In Fig. 3, the 'good' estimates of offset completely sample the range of sensor temperature, T_S, in spite of lack of good estimates within the ROI (Fig. 1).
- A smoothing spline is found by performing linear regression on 1°C bins, yielding temperature dependence functions $o_1(T_S)$ and $o_2(T_S)$.
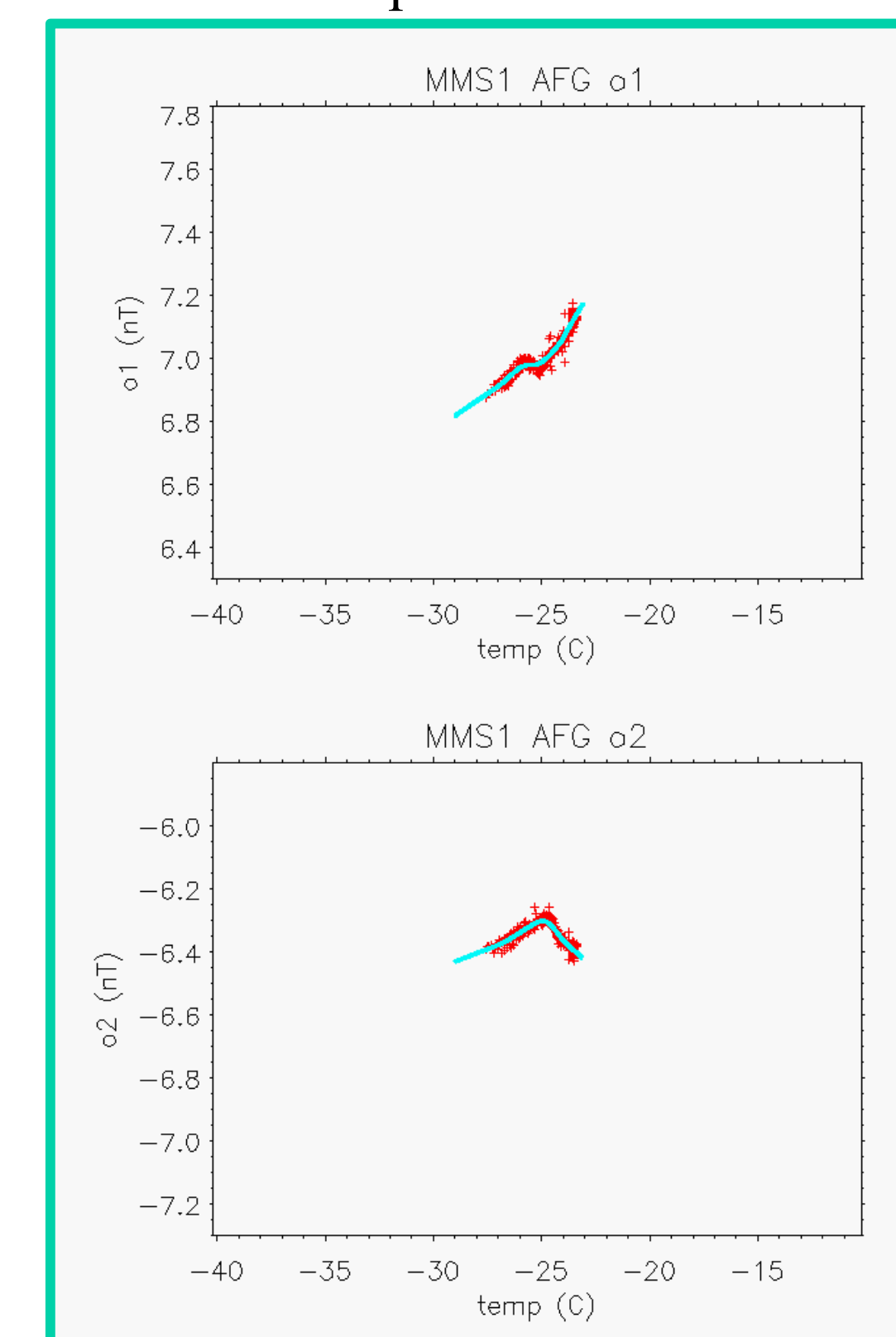
Time Evolution of Temperature Dependence

Two distinct modes of change:

1) Gradual Evolution:
   - The shape the the functions $o_1(T_S)$ and $o_2(T_S)$ evolve on a timescale ≥ 7 orbits.
   - Compare Fig. 3 with the left two panels of Fig. 4, which show the temperature dependence of the same sensors after 4 months of continued evolution.

2) Discrete Jumps (occasional, ~several months)
   - Random, discrete jumps of 0.1 – 0.2 nT typically occur near perigee, while in high-field range.
   - Other jumps are associated with maneuvers.
   - Interestingly, these sudden jumps do not alter the shape of the temperature dependence function, as seen the bottom right panel of Fig. 4.
   - The offsets from orbits before and after such jumps can be normalized to obtain a single temperature dependence function (Fig. 4).

Fig. 3. Dynamic offsets (red) for 7 orbits from Phase 1A (see Fig. 1) plotted with respect to Sensor Temperature, with spline fit (cyan).
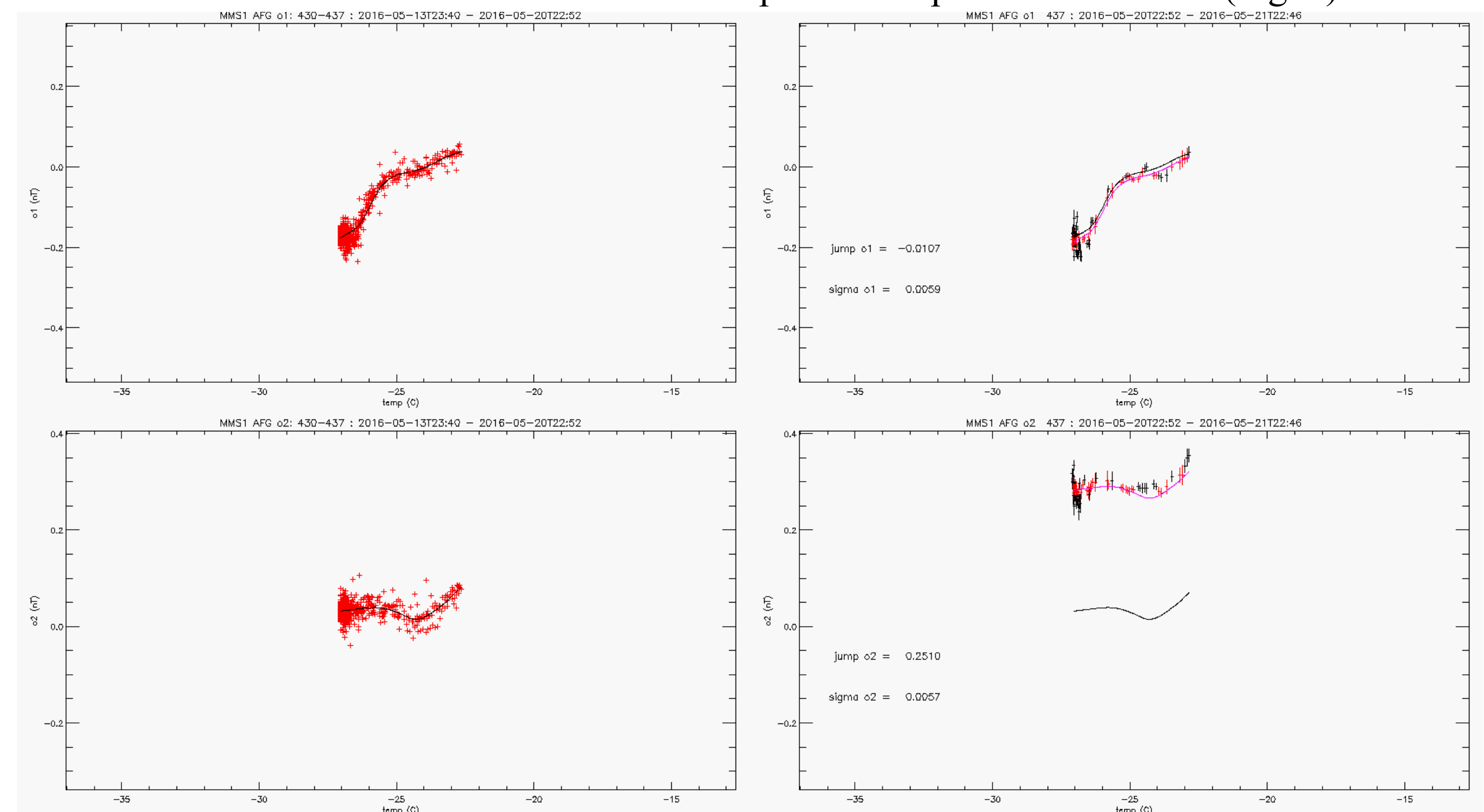

Fig. 4. On the left: normalized dynamic offsets (red) for 7 orbits, with spline fit (black), which is repeated on the right, compared to normalized dynamic offsets (red and black) for the following orbit, assuming no change in normalization. The red curve shows the same spline, after normalization to the new orbit; red + indicates middle 50 percentile.

Temperature Dependence, contd.

Temperature Dependence During Eclipse – Comparison of All Instruments

During the eclipse season, the temperature dependence is no longer single-valued.

- The time intervals are separated according to $dT_S(t)/dt$. (c.f. Fig. 4), yielding two distinct temperature dependence functions (Fig. 5) for each sensor axis, i:
  1. $o_i^A(T_S)$ where $dT_S(t)/dt \geq$ -0.0005 °C/s: 'Adiabatic' temperature recovery
     - Gradually increasing temperature during Eclipse Recovery.
     - Slowly decreasing temperature (e.g. cooling after Earth's albedo, as in Fig. 4)
     - These time intervals are often in the ROI, and may affect primary science.
  2. $o_i^E(T_S)$ where $dT_S(t)/dt <$ -0.0005 °C/s: Eclipse / rapid cooling
     - Use adaptable bin size for linear regressions to obtain at least 15 points per bin.
     - No science requirement during eclipse; however, calibrations can still be improved.
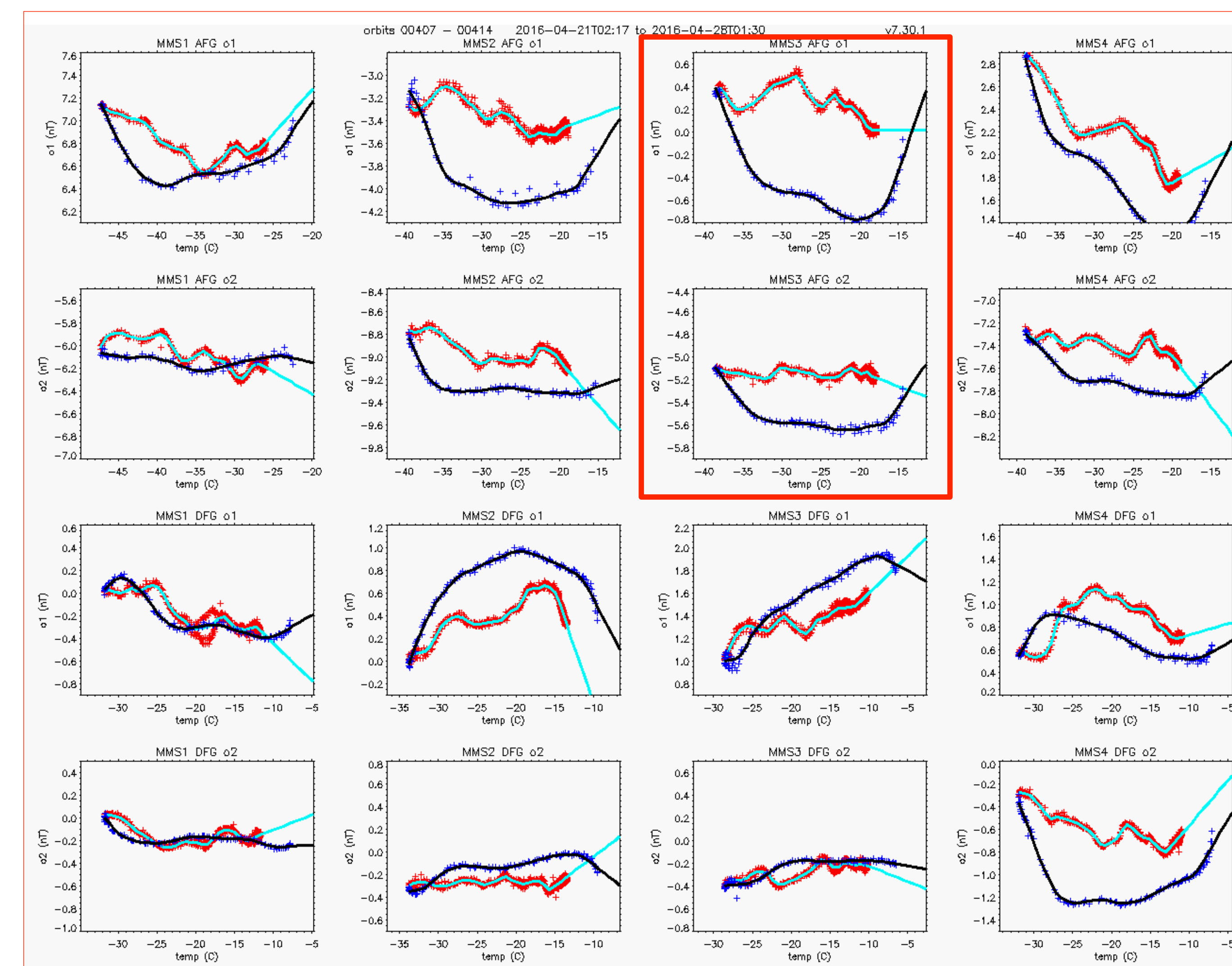

Fig. 5. Each spin-plane sensor of the 8 MMS FGM instruments has a distinct temperature dependence function. Our Phase 1X example from Fig. 2 is MMS3 AFG (outlined in red). Red + : intervals of 'adiabatic' temperature change; Blue + : eclipse.

Application on the Nightside

- On a 7-orbit cadence, determine temperature splines $o_i^A(T_S)$ for each sensor axis, i.
- If there are eclipses, also determine $o_i^E(T_S)$
- These are then mapped back into the time domain using the measured sensor temperatures, $T_S(t)$.
  - Let E be the set of times for which $dT_S(t)/dt <$ -0.0005 °C/s.
  - For each sensor axis, i, define a function of offset with respect to time, $o_i(t)$, which is continuous except for minor discontinuities upon eclipse entry/exit:

$$o_i(t) = \begin{cases} o_i^A(T_S(t)) & \text{for} \quad t \notin E \\ o_i^E(T_S(t)) & \text{for} \quad t \in E \end{cases}$$

- A superposed epoch analysis (Fig. 6 and Fig. 7) provides a detailed view of the result, revealing the repeatability of the offset changes on each of the 7 orbits. (Minimum sensor temperature determines Epoch 00:00.)
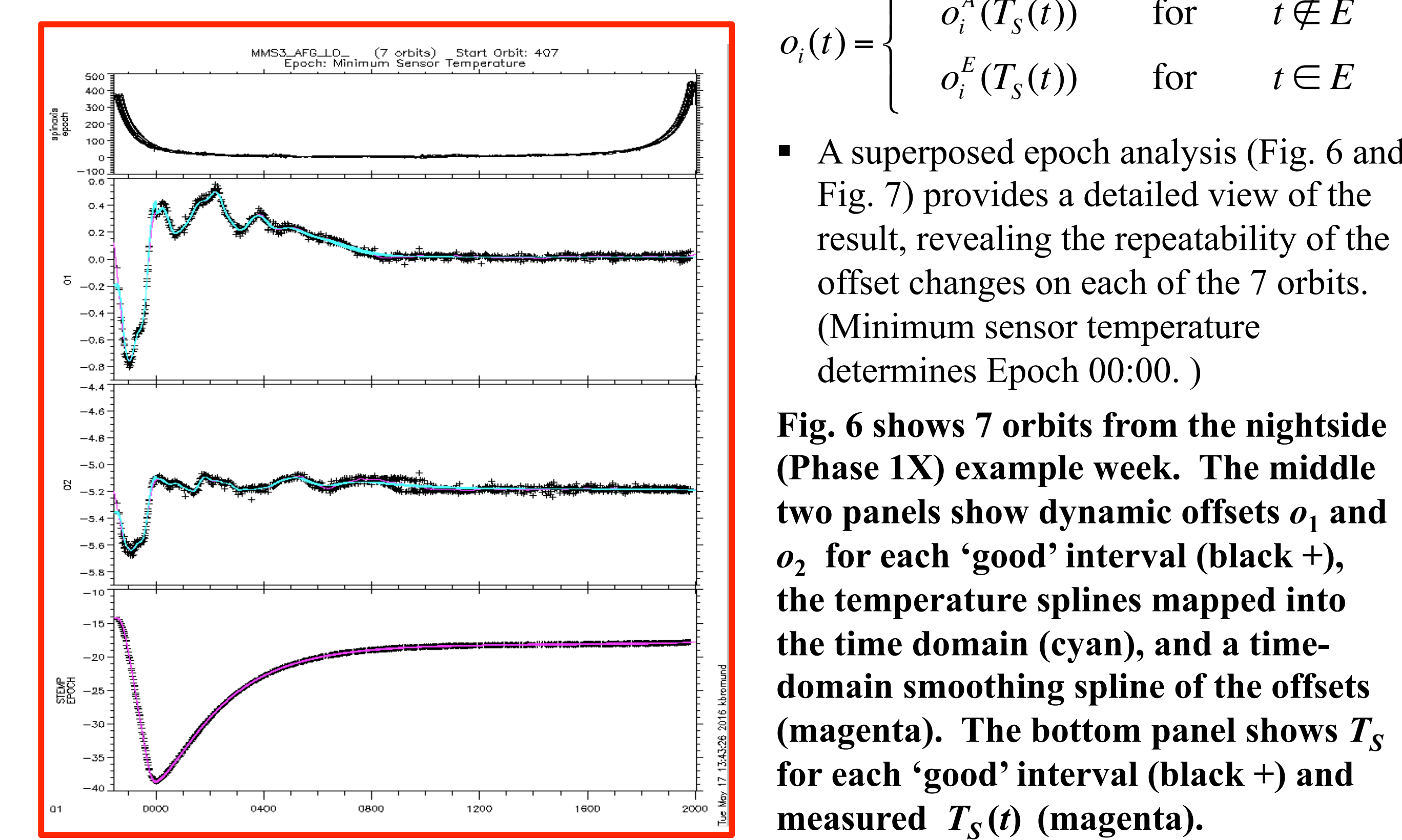
Fig. 6 shows 7 orbits from the nightside (Phase 1X) example week. The middle two panels show dynamic offsets o_1 and o_2 for each 'good' interval (black +), the temperature splines mapped into the time domain (cyan), and a time-domain smoothing spline of the offsets (magenta). The bottom panel shows T_S for each 'good' interval (black +) and measured $T_S(t)$ (magenta).
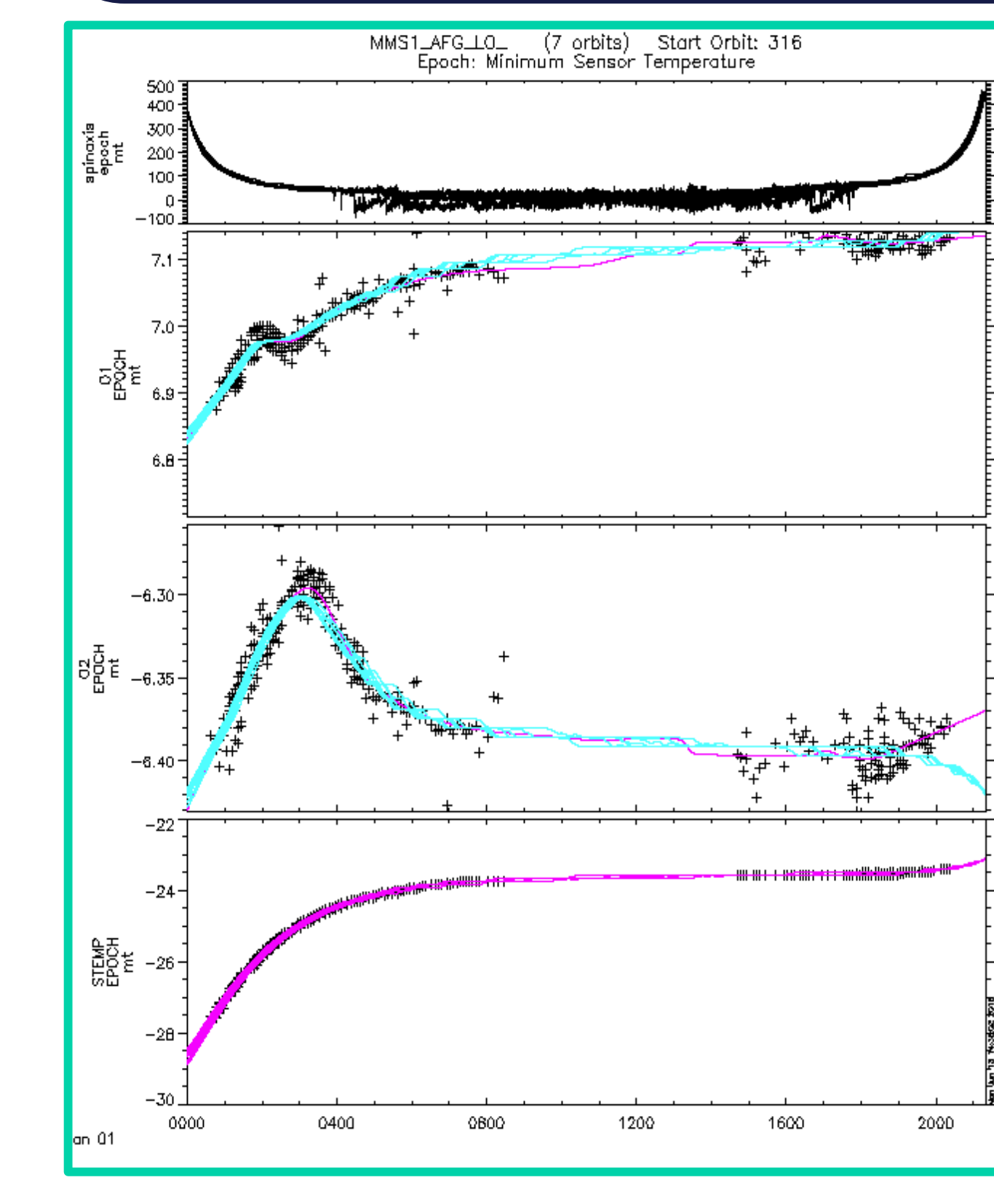
Application on the Dayside

Fig. 7. Superposed epoch of 7 orbits from the dayside (Phase 1A) example week. The middle two panels show dynamic offsets o_1 and o_2 for each 'good' interval (black +), the temperature splines mapped into the time domain (cyan), and a time-domain smoothing spline of the offsets (magenta). The bottom panel shows T_S for each 'good' interval (black +) and measured $T_S(t)$ (magenta).

- The new method gives the ability to determine offsets in the ROI, even when there are no reliable offset measurements within the ROI.
- Allows significant improvement for cases when offset changes from one orbit to next.
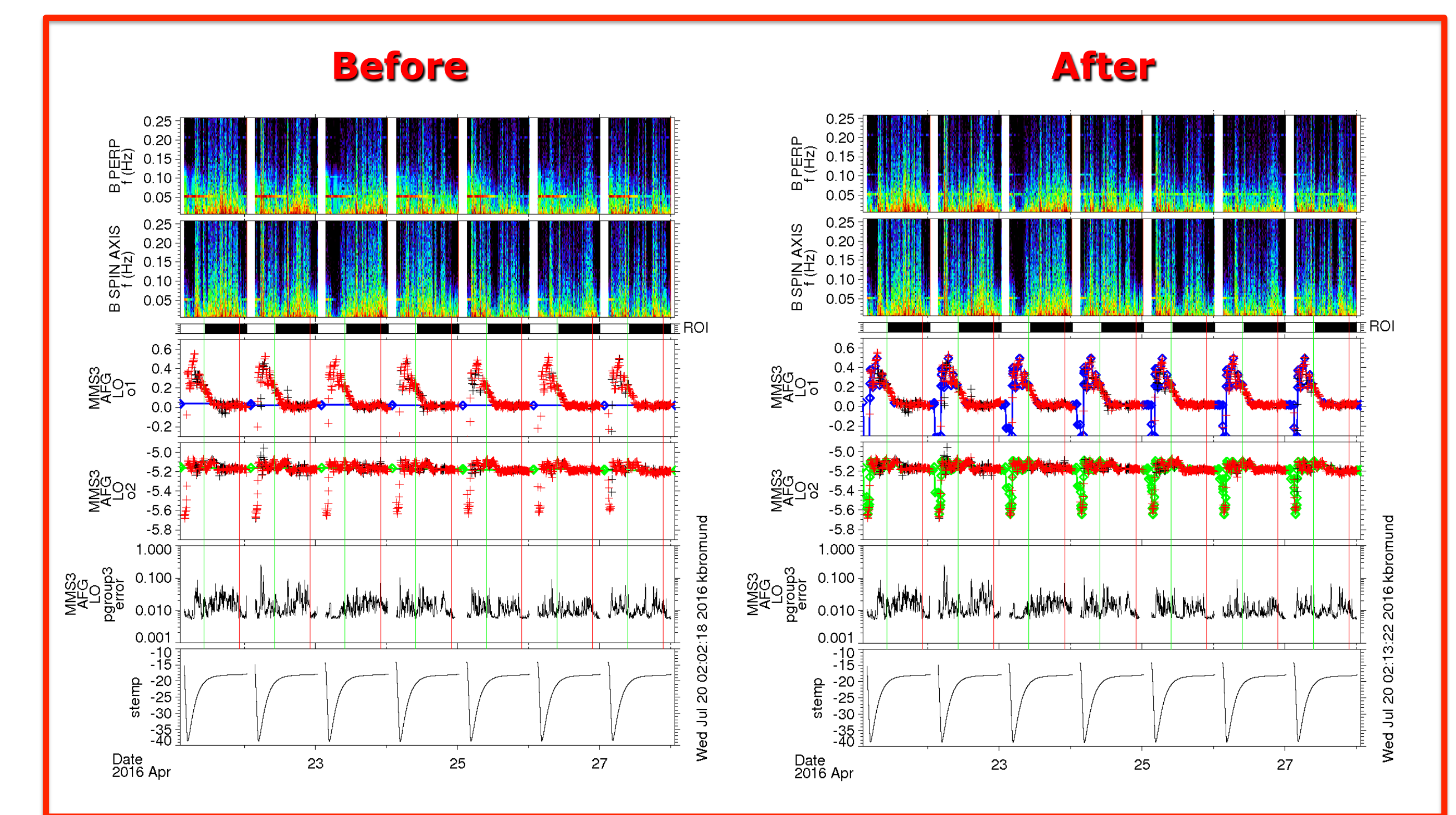
Results

Before   **After**

Fig. 8. Constant offsets (detail of Fig. 2, left) are replaced by dynamic offsets (right) for the nightside (Phase 1X) example. Typically, < 10 extra entries in the calibration tables are necessary per orbit in order to maintain fidelity of ≤ 10 pT to the temperature-dependent offset functions, $o_i(t)$ (Fig. 6).

Discussion

- Offsets change with temperature in a quasi-deterministic and repeatable manner. At time scales of about 7 orbits, temperature dependence curves are well defined.
- Each spin-plane sensor has a distinct temperature-offset curve.
  - It is likely that the spin-axis sensors exhibit similar temperature dependence, although the current methods cannot measure or correct the spin axis offset.
  - If left uncorrected, there are implications for inter-spacecraft data analysis, particularly in Phase 2, where changes may persist after eclipse for up to 12 hours in the ROI.
- The new method typically corrects spin-plane offsets to better than 50 pT in the ROI.
- The new algorithms are in place for Phase 2.
  - The temperature-dependent offset correction is in production for L2pre and L2 as of orbit 479 (2016-07-01 18:07). This includes most of the Phase 1X season of long eclipses.
  - Refinement to account for discrete jumps is in production as of 2016-11-18 01:52
- Future work:
  - Re-process L2 data to correct the remainder of Phase 1X and before.
  - Investigate methods to reveal short-term temperature dependence of spin-axis offset.

References

Bromund, Leinweber, Plaschke, et al. (2015), "In-Flight Calibration Processes for the MMS Fluxgate Magnetometers," Abstract SM51A-2555 presented at 2016 Fall Meeting, San Francisco

Russell, et al. (2014). "The Magnetospheric Multiscale Magnetometers." Space Sci Rev.; DOI: 10.1007/s11214-014-0057-3